Enhanced hemocompatibility of Lysine grafted polyacrylonitrile electrospun nanofiber membranes as a potential bilirubin adsorption in hemoperfusion

Muhua Liu
Tiangong University
Wen Zhang (zhangwen2050@hotmail.com)
Tiangong University https://orcid.org/0000-0001-9739-9799
Hao Li
Tiangong University
Jinjie Zhan
Tiangong University
Wenjun Zhao
Tiangong University
Xi Mei
Tiangong University

Research Article

Keywords: Electrospun nanofiber membranes, polyacrylonitrile, lysine, bilirubin, adsorption, hemocompatibility

Posted Date: June 7th, 2022

DOI: https://doi.org/10.21203/rs.3.rs-1641065/v1

Enhanced hemocompatibility of Lysine grafted polyacrylonitrile electrospun nanofiber membranes as a potential bilirubin adsorption in hemoperfusion

Muhua Liu[a]·Wen Zhang[a,*]·Hao Li[a]·Jinjie Zhan[a]·Wenjun Zhao[a]·Xi Mei[a]

[a]State Key Laboratory of Separation Membranes and Membrane Processes, School of Material Science and Engineering, Tian Gong University, Tianjin 300387, China
[*]Corresponding author. E-mail address: zhangwen2050@hotmail.com, Tel.: +86 13516155156

Abstract

Hyperbilirubinemia is one of most severe clinical diseases, which is caused by the accumulation of unconjugated bilirubin. Electrospun nanofiber membranes used as highly efficient bilirubin adsorbents have been applied to remove the extra bilirubin in hemoperfusion for their high surface area and easy functionalized properties. In this work, Lysine (Lys) grafted polyacrylonitrile (PAN) electrospun nanofiber membranes doped with organic Hectorite (OHec) (Lys-HPAN@OHec) have been fabricated via a series of modified process, including pore forming, alkaline hydrolysis and grafting reaction. The obtained Lys-HPAN@OHec nanofiber membranes have been analyzed in detail and investigated the adsorption capacity for bilirubin. Compared with original PNA membranes, Lys-HPAN@OHec nanofiber membranes show an excellent bilirubin adsorption capacity and more stable rejection rate of bovine serum albumin (BSA). The maximum adsorption capacity of Lys-HPAN@OHec membranes for bilirubin is 64 mg/g, the adsorption process of Lys-HPAN@OHec membranes matched the Langmuir model well. In addition, dynamic adsorption reveals that the adsorption equilibrium time of Lys-HPAN@OHec membranes is about 2 h. Significantly, Lys-HPAN@OHec membranes have excellent biocompatibility and hemocompatibility. This study demonstrates that the novel Lys-HPAN@OHec membranes may provide a new way to treat hyperbilirubinemia.

Keywords: Electrospun nanofiber membranes · polyacrylonitrile · lysine · bilirubin · adsorption · hemocompatibility

Introduction

Hyperbilirubinemia, one of the most common problems, will be encountered when bilirubin accumulates in the blood over the normal level, especially for newborns [1]. It is well known that hyperbilirubinemia can cause some severe diseases, such as jaundice, hepatitis, and even irreversible brain damage [2, 3]. Nowadays, intensive researchers devote themselves to find the most efficient way to remove bilirubin from the patients. Photo-therapy, hemodialysis, or hemoperfusion can purify blood by removing excessive bilirubin or toxins in the body and has already been developed to decrease free bilirubin from plasma within the normal range [4]. Among them, hemoperfusion treatment refers to the circulation of blood through an extracorporeal unit which contains an adsorbent device for endogenous or exogenous pathogenic substances in blood [5]. Materials based hemoperfusion have been developed and applied for bilirubin removal, including as activated carbon [6], mesoporous materials [7], inorganic or organic particles [8, 9], nanofiber membranes [10], etc. It should be stressed in particular that electrospun nanofiber membranes have been extensively utilized for blood purification materials because of their high porosity, high surface area, easy modification or degradation property.

As well known, polyacrylonitrile (PAN), one of the most important polymers, is suitable to be electrospun into nanofibers [11], due to its good spinnability, chemical/physical stability, mechanical property and hydrophobicity. However, pure PAN has high degree of hydrophobicity and relatively poor biocompatibility which limits it to be used in biomedical applications [12]. The relevant literature show that the surface modification of PAN nanofiber membranes has been used widely to improve their properties [13, 14], which will expand the application fields and have great potential to be used in hemoperfusion. In group of Jiang [15], shape-controlled palladium nanoparticle-decorated electrospun polypyrrole/polyacrylonitrile nanofibers (Pd_PPy/PAN NFs) were fabricated by vapor deposition polymerization and

electrodeposition. The results revealed that Pd_PPy/PAN NFs could be used as monitoring diseases related to H_2O_2 concentration, such as Parkinson's disease or Alzheimer's disease. As a promising and biocompatible ploymer, branched polyethylenimine (bPEI) has been widely applied in the biological field, such as gene delivery [16]. By means of a green hydrothermal process, Zhao et al. fabricated bPEI grafted electrospun PAN fiber membrane (bPEIPANFM) and investigated the adsorption performance toward bilirubin [10], and bPEIPANFM showed the best removal ability for bilirubin, excellent biocompatibility and hemocompatibility. Bilirubin molecule contains carboxyl and amino groups, hence bilirubin can be removed through electrostatic interactions and/or hydrogen bonding by the absorbents containing amino and hydroxyl groups [17, 18]. For example, Jiang et al. [19] reported that the functional polyethersulfone/poly (glycidyl methacrylate) hybrid particles modified by four kinds of amine reagents were used for the removal of bilirubin. Results demonstrated that the particles performed well in the adsorption of bilirubin, promising its potential application in the fields of hemoperfusion treatment. In addition, functionalized poly(vinyl alcohol-co-ethylene) (PVA-co-PE) nanofibrous membranes were prepared with different amine compounds, the best adsorption capacity for bilirubin of diethylenetriamine functionalized nanofibrous membranes could reach 110 mg/g [20].

In addition, bovine serum albumin (BSA) was usually introduced into the adsorbent for bilirubin removal due to the intensive interaction between molecules. As reported, BSA molecules could form a strong complex with bilirubin providing a great increase in adsorption capacity for bilirubin [21]. Hence, BSA was immobilized on the surface of polyethersulfone/polydopamine (PES/PDA) electrospun fiber mat to selectively remove bilirubin [22]. The adsorption experiments demonstrated that PES/PDA-BSA had an excellent adsorption capacity and a good selectivity. Shi and his colleagues fabricated poly-L-lysine containing nylon micro-filtration membranes for bilirubin adsorption, and experiments showed that the adsorption mechanism of PLL-attached membranes was a monolayer adsorption [23]. Besides, the literature reported that lysine (Lys) grafted PAN fiber exhibited highly catalytic activity for

Knoevenagel condensation reaction [24]. However, Lys grafted electrospun PAN fibers have not been reported yet.

In this study, we reported the fabrication of Lys grafted PAN nanofiber membranes via a novel and facile procedure. Poly(4-vinylpyridine) (PVP) and organic Hectorite (OHec) were doped with spinning solution to obtain the modified PAN@OHec membranes. Lys was grafted on the surface of PAN@OHec (Lys-HPAN@OHec) membranes via alkaline hydrolysis and grafting reaction. The obtained Lys-HPAN@OHec nanofiber membranes had been analyzed in detail and investigated the adsorption capacity for bilirubin.

Materials and methods

Materials

L-Lys (≥98%), bilirubin (≥98%), BSA (≥98%) and 3-(4, 5-dimethylthiazol-2-yl)-2, 5-diphenyl tetrazolium bromide (MTT) were received from Aladdin reagent Co. Ltd. (China). 1-ethyl-(3-dimethylaminopropyl) carbodiimide hydrochloride (EDC, ≥99%) and N-hydroxysuccinimide (NHS, ≥99%) were obtained from Shanghai Civic Chemical Technology Co, Ltd. Hectorite (Hec) was purchased from British Lockwood Auxiliary Company. PAN (Mw~50,000) was purchased from Jilin Petrochemical Company. PVP, N, N-dimethylformamide (DMF, ≥99%) and cetyltrimethylammonium bromide (CTAB) were purchased from Tianjin Guangfu Fine Chemical Research Institute.

Electrospinning of PAN@OHec Nanofibers Membrane

Hec was modified with CTAB through ion exchange method [25], and organic Hec (OHec) was synthesized for next step. PAN@OHec nanofiber membranes were composed of PAN (1.5 g), PVP (1.0 g), OHec (0.6 g) and DMF (10 mL), and prepared according to the literature method [26]. Electrospinning solution was prepared by 15 wt% PAN dissolved in DMF. PVP and OHec were added to above solution, and then mechanical stirring was used for 12 h at room temperature to obtain homogeneous solution. The prepared solution was added to a 10 mL glass syringe

with a needle tip (0.5 mm diameter) and then electrospun under a voltage of 23 kV. The feeding rate of the polymer solution was 1 mL/h and the distance from the tip to the collector was 15 cm. Then PAN@OHec nanofiber membrane was soaked in distilled water for 4 h to remove excess PVP and dried in an air-circulating oven at 60 ^{o}C for 24 h.

Fabrication of Lys-HPAN@OHec Nanofibers Membrane

The hydrolysis of PAN@OHec nanofiber membrane was performed with NaOH. 1 g of the nanofiber membranes were immersed in different concentration of NaOH solution and stirred at 45 ^{o}C for various periods. Afterwards, the hydrolyzed nanofiber membranes were continuously washed with distilled water and dried at 50 ^{o}C for 48h. Above prepared membranes were designated as HPAN@OHec nanofiber membranes.

A typical procedure of the grafting reaction of HPAN@OHec and Lys was described as follows (see Scheme 1). HPAN@OHec nanofiber membranes (1.0 g) were immersed in a mixture of EDC (1.189 g), NHS (0.238 g), Lys (1.08 g) and 100 mL of distilled water in a breaker and stirred for 12 h at 30 ^{o}C. After reaction, the resulting nanofiber membranes were placed in a dialyzed bag in distilled water to remove the remaining reagents and by-products. Then the nanofiber membranes were immersed in 18 wt% PEG solution for 24 h at room temperature. The obtained nanofiber membranes were freeze-dried and named as Lys-HPAN@OHec nanofiber membranes.

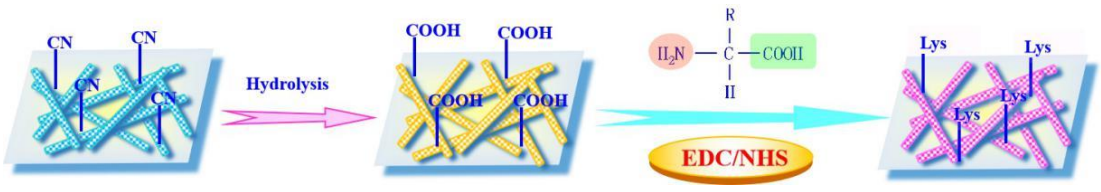

Scheme 1. Fabrication process of Lys-HPAN@OHec nanofiber membrane.

Membranes characterization

The morphology of nanofiber membranes were investigated by using a field emission scanning electron microscope (FE-SEM, JSM-7500F, Tokyo, Japan). Elemental analysis of the samples was obtained through an Energy Dispersive X-Ray

spectroscopy (EDX, INC250, Japan Electronic). Fourier transform infrared (FT-IR) spectra were examined with the FT-IR spectroscopy (Tensor 37, Bruker, Germany). All spectra were obtained in the range of 400~4000 cm^{-1} using KBr pellet method. Surface chemical characterization was performed by X-ray photoelectron spectroscopy (XPS) using a Bruker AXS Discover D8 with Al/Kα (hν = 1,486.6 eV) anode mono X-ray source. By measuring the flowing current or flowing a voltage on the solid surface, zeta potential was calculated as vital information of the material.

Fouling tests of the membranes

(1) Protein adsorption

The adsorption of protein was carried out with BSA solution under static conditions. The 50 mg virgin membranes and Lys-HPAN@OHec membranes were immersed into BSA solution (0.1 mg/mL) and incubated for 2 h, at 37 °C. Each membranes were washed using PBS in order to remove the unadsorbed proteins. The absorbance of BSA solutions was measured by a UV-vis spectrometer (UV- 2000, Shimadzu, Japan) at 280 nm. Each test was performed three times on each membrane. The BSA adsorption of the membranes was calculated based on the change in the solution concentration.

(2) Protein fouling property

Protein fouling tests were carried out at room temperature using the dynamic experiments. Before fouling tests, the membranes were performed to attain a stable water flux (J_0). Then, the protein flux of the membranes were recorded under the operating pressure of 0.02 MPa with BSA solution, the water or protein flux was calculated by the following Equ (1).

$$J = \frac{V}{A \cdot t} \tag{1}$$

where J is the water permeation flux of the membrane ($L \cdot m^{-2} \cdot h^{-1}$), A is the effective area of the membrane (m^2), V is the volume of permeate pure water (L), and t is the operation time (h), respectively.

Adsorption for bilirubin of the membranes

(1) Adsorption of bilirubin

It was discovered that bilirubin was susceptive to light and easily decomposed, the adsorption experiments should be performed with treatment of light avoidance. Firstly, bilirubin (stored in dark at -20 ºC) was dissolved in 0.1 M NaOH solution and diluted with PBS (pH = 7.4), and then bilirubin solution with varied concentrations were prepared to next experiments. The above solution was filtered to remove solid bilirubin if any remained and also stored in dark. The adsorption properties of samples were investigated at dynamic and static conditions, respectively. All the bilirubin solution was used immediately after preparation.

(2) Adsorption dynamics

50 mg of samples were applied in 10 mL bilirubin solution at 25 ºC with oscillation. The concentration was determined at predetermined time intervals by a UV-vis spectrometer at 438 nm. Results are expressed with 95% confidence intervals. The amount of adsorption q (mg/g) was calculated by the following Equ (2).

$$q = \frac{(C_0 - C) \cdot V}{m} \tag{2}$$

where C_o and C are the initial and the residual bilirubin concentration in solution (mg/mL), V (mL) is the volume of bilirubin solution, m (mg) is the mass of the adsorbent, respectively.

(3) Adsorption isotherm

In the adsorption isotherm experiment, 20 mg of samples were added into a 50-mL tube and suspended in distilled water with specific initial bilirubin concentration ranging from 100 to 300 mg/L. The tube was sealed and shaken for 24 h at 25 ºC and 37 ºC. The adsorption amount of bilirubin was determined by the method as mentioned above. In addition, the adsorption isotherms should be fitted with Langmuir model and Freundlich mode, respectively. All of the adsorption experiments were performed in triplicates.

The Langmuir model could be used for describing the monolayer adsorption based on the assumption of adsorption homogeneity. Nevertheless, the Freundlich model was empirical, which was assumed the adsorption process take place on a heterogeneous surface. Moreover, the Freundlich model was an empirical equation that assumes a heterogeneous surface energy and described the multilayer adsorption. The calculation formulas of two models were expressed by the following Eqn (3) and (4), respectively.

$$\frac{C_e}{q_e} = \frac{1}{K_L q_m} + \frac{C_e}{q_m} \tag{3}$$

$$\ln q_e = \ln K_F + \frac{1}{n} \ln C_e \tag{4}$$

where C_e (mg/mL) is the bilirubin concentration at equilibrium condition, q_e (mg/g) is the equilibrium adsorption capacity, and q_m (mg/g) is the maximum adsorption in line with the Langmuir model. K_L (L/mg) is the Langmuir adsorption constant, and K_F (mg/g) is the Freundlich adsorption constant. n is a Freundlich linearity index, 1/n represents the intensity of the adsorption.

Cytocompatibility and hemocompatibility

(1) Cell viability assay

L929 fibroblast cells (1.0×10^4 cells/well) were seeded into 96-well plate at 37°C in 5% CO_2 for 24 h prior to the test. The leaching liquor of all membranes was added to 96-well plate with different concentrations and incubated for 1, 3, or 5 days, and the plate without leaching liquor was as the blank control. At specific time intervals of cultivation, the cytotoxicity of the membranes was evaluated by MTT assay. The absorbance was measured at 490 nm using a microplate reader (MK3, Thermo, USA). The cell viability was expressed as a percentage compared to the control. Observation of cells adhering to the membranes was performed with an inverted microscope (Nikon, TS100, Japan).

(2) Coagulation assay

Platelet poor plasma (PPP) was obtained from the blood sample of a healthy adult volunteer by centrifuging for 15 min. PAN or Lys-HPAN@OHec membranes were incubated in PPP (2 mL) at 37 °C for 30 min. Then, the supernatant liquor of each sample was measured three times to analyze the mean values of activated partial thromboplastin time (APTT), prothrombin time (PT) and thrombin time (TT) with an automatic coagulation analyzer (Kobe, Sysmes, Japan), respectively.

(3) Hemolysis assay

Fresh blood was centrifuged at 1000 rpm for 15 min to collect the bottom layer of erythrocyte. For the hemolysis test, 10 mg of the membranes were washed with distilled water and physiologic saline, and then immersed in 10 mL saline solution for 30 min in centrifugal tube. 200 μL of fresh erythrocyte was added to the tube and incubated at 37 °C for 60 min. The 200 μL fresh erythrocyte were incubated in 10 mL PBS solution as negative control, and 10 mL distilled water as positive control. The mixture were centrifuged for 10 min at 1000 rpm, and the absorbance of th supernatant was measured at 540 nm using a UV-vis spectrometer. The hemolysis ratio was calculated as follows Eqn (5),

$$Hemolysis\ ratio\ (\%) = \frac{OD_s - OD_{nc}}{OD_{pc} - OD_{nc}} \times 100\% \quad (5)$$

where OD_s, OD_{pc} and OD_{nc} are the absorbances of the sample, positive control, and negative control, respectively.

Results and discussion

Optimize the hydrolysis process

The effect of the hydrolysis condition on the morphology and structure of PAN nanofiber membranes were discussed and shown in Fig. 1 and 2. SEM results revealed that the reaction time and NaOH concentration had a great influence on the morphology of PAN nanofiber membranes. The diameter of nanofiber increased with the increasing of the reaction time from 1h to 5h (Fig. 1a-c). Meanwhile, it was found that the effect of NaOH concentration on the morphology followed the same trend in

Fig. 1d-f. However, there was obviously surface adhesion between nanofibers when the concentration of NaOH solution was 2.5 mol/L. The swelling of nanofibers could occur and lead to the increase of fiber diameter in the hydrolysis process [27].

The FT-IR spectra of PAN nanofiber membranes hydrolyzed under various conditions were shown and compared in Fig. 2. The peak located at 2242 cm^{-1} in Fig. 2a could be attributed to C≡N group of PAN nanofibers [28]. The intensity of this band decreased after participating the hydrolysis reaction. However, this peak didn't disappear completely, which mean that partial nitrile group are hydrolyzed. The band observed at 1659 cm^{-1} was associated with C=O stretching of the amide groups, the bands at 1569 and 1410 cm^{-1} were assigned to the combined vibrations of carboxylate (COO-) and imine conjugated sequences (-C=N-) [29, 30]. Above bands were just observed in FT-IR of hydrolyzed PAN. The broad peak at 3750~3200 cm^{-1} were resulted from the hydrolysis of the acetate groups. The hydrolysis increased with the increasing NaOH concentration and reaction time in Fig. 2. Therefore, PAN nanofiber membranes could be hydrolyzed for 3h with 2 mol/L NaOH solution in order to be the optimum.

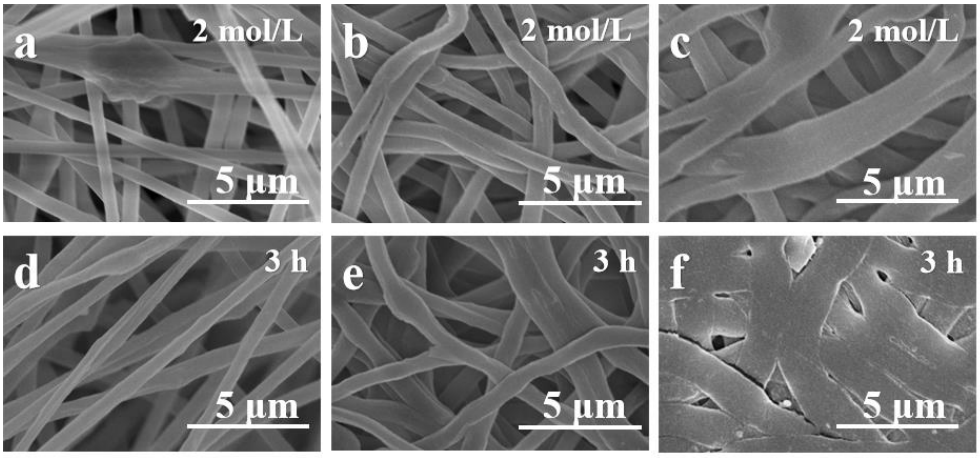

Fig. 1 SEM images of electrospun PAN membranes hydrolyzed for different time (a-c) with various NaOH solution (d-f), 1 h (a), 3 h (b), 5 h (c), 1 mol/L (d), 2 mol/L (e) and 2.5 mol/L (f).

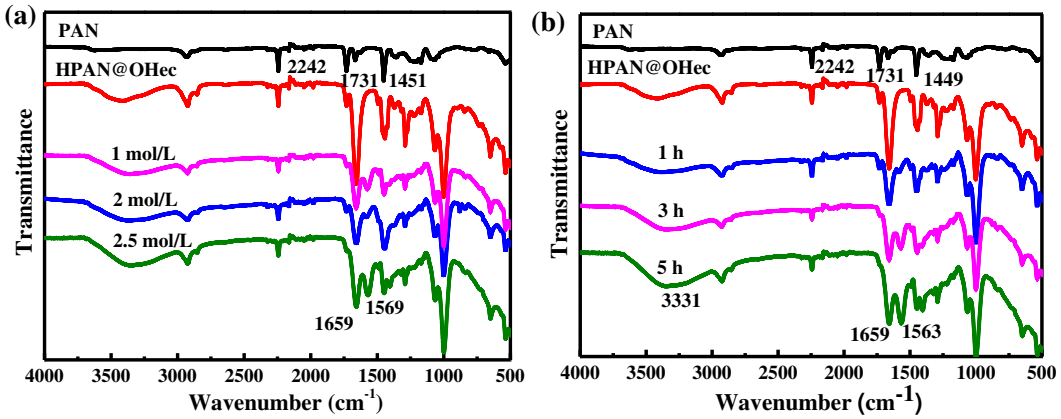

Fig. 2 Effect of the NaOH concentration (a) and the reaction time (b) on the FT-IR spectra of electrospun PAN membranes

Membrane characterization

Fig. 3 showed the morphology of raw PAN, PAN@OHec, HPAN@OHec and Lys-HPAN@OHec nanofiber membranes. It was obviously seen that the surface of raw PAN membranes was smooth and compact. As seen from Fig. 3b-d, the diameter and the surface roughness of membranes all increased which may be due to the pore-forming action of PVP and the grafting of Lys onto the surface of membranes. The diameter of PAN@OHec membranes after hydrolysis with NaOH increased to 640 nm, which may be due to the swelling and expansion of hydrolyzed membranes. Compared with the raw PAN membranes, the average diameter of Lys-HPAN@OHec was about twice that of the raw PAN membranes and the roughness was about three times (seen in Fig. 4).

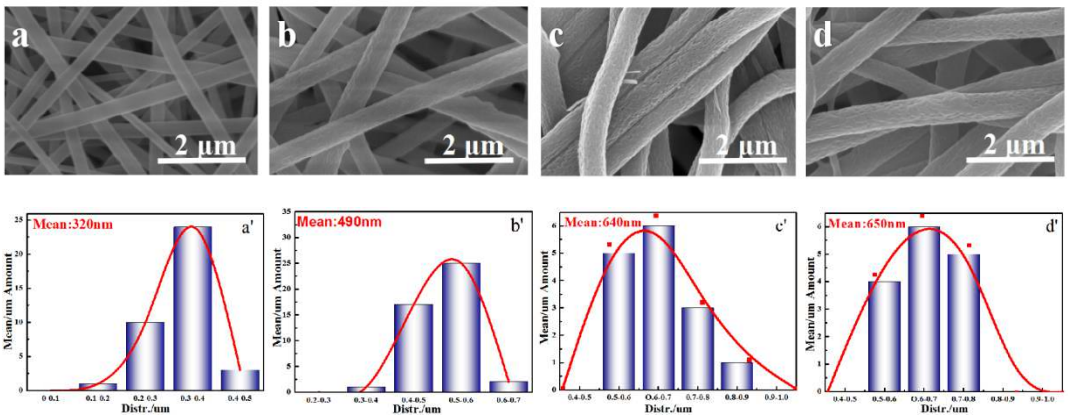

Fig. 3 SEM images (a-d) and the diameter distribution (a'-d') of PAN, PAN@OHec, HPAN@OHec and Lys-HPAN@OHec.

The FT-IR spectra of Lys-HPAN@OHec nanofiber membranes were shown in Fig. 5a. The 2242 cm^{-1} absorption band of Lys-HPAN@OHec membranes was attributed to C≡N vibrations and the intensity of this band decreased after hydrolysis. It was illustrated that some C≡N groups converted into -COOH groups in the process of reaction. Compared with PAN membranes, the new bands at 1662 cm^{-1}, 1651 cm^{-1}, 1563 cm^{-1} and 1401 cm^{-1} occurred in the spectrum of Lys-HPAN@OHec. The band at 1662 cm^{-1} was attributed to C=O stretching of the amide. The 1655 cm^{-1} peak was resulted from the stretching vibration of C=O in Lys, which indicate the successful grafting of the Lys on the surface of modified membranes [24].

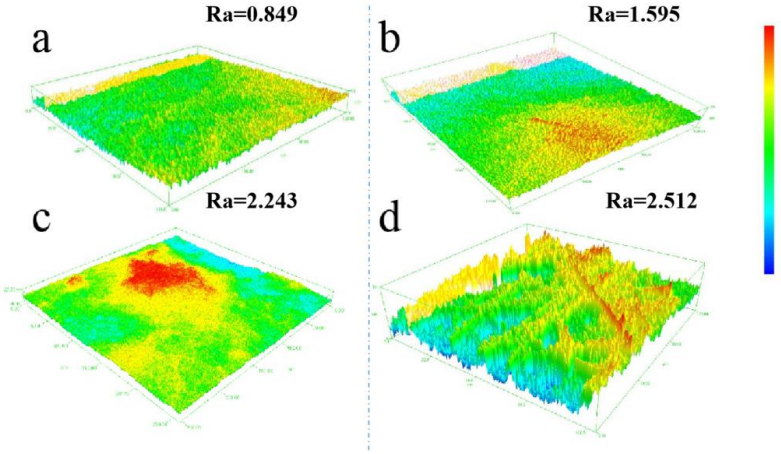

Fig. 4 True Colour Confocal Microscope images (a-d) of PAN, PAN@OHec, HPAN@OHec and Lys-HPAN@OHec.

XPS analysis is used to further clarify the surface chemical composition of the membranes and XPS spectra is recorded and presented in Fig. 5b. The peaks at 285.1, 399.2 and 531.2 eV were found in the XPS full-scan spectra of the membranes and resulted from C1s, O1s and N1s, respectively. The O1s peaks could be deconvoluted to two peaks at 530.28 and 531.18eV (Fig. 5c), which attribute to C=O and -OH [31]. For the N 1s spectrum of Lys-HPAN@OHec (Fig. 5d), the peak at 399.2 eV was attributed to C≡N, NH_2 or NH groups [32], respectively. These groups indicated that Lys would be successful grafted onto the HPAN@OHec membranes. Moreover, above result was consistent with the FT-IR analysis.

As seen from Fig. 6, the porosity, hydrophilic and surface potential of various membranes were recorded and shown, respectively. Compared with the pure PAN

membranes, the porosity of the modified membranes increased from 35% to about 80 % (Fig. 6a). And the reason why it could be increased that PVP as the porogen could change the surface morphology of membranes and produce a large amount of microvoids.

Meanwhile, the surface properties of PAN and modified membranes were characterized by water contact angle and surface charge measurements in Fig.6b, c. The pure PAN membranes exhibited excellent hydrophobicity and the water contact angle was about 135° . However, the water contact angles of the modified PAN membranes after pore-forming and hydrolysis occurring were obviously decreased. The water contact angle of Lys-HPAN@OHec membranes was as high as 23° at 1s and the complete infiltration time was only 2s. This was because that the hydrophilic groups, such as carboxy groups or the amide bonds, could increase the interaction between membranes and water. Hence, the modified membranes exhibited good hydrophilicity.

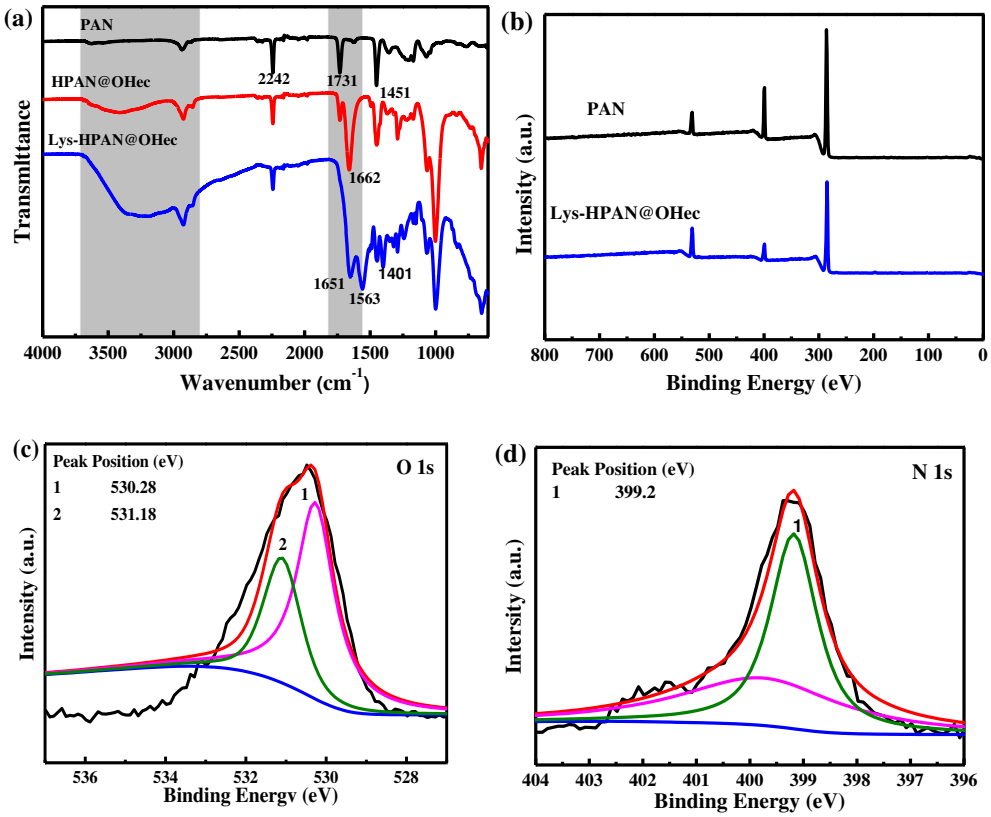

Fig.5 The FT-IR spectra of the PAN, HPAN@OHec and Lys-HPAN@OHec (a), Survey XPS spectra of PAN and Lys-HPAN@OHec (b), O1s core level spectra (c) and N1s core level spectra (d) of Lys-HPAN@OHec.

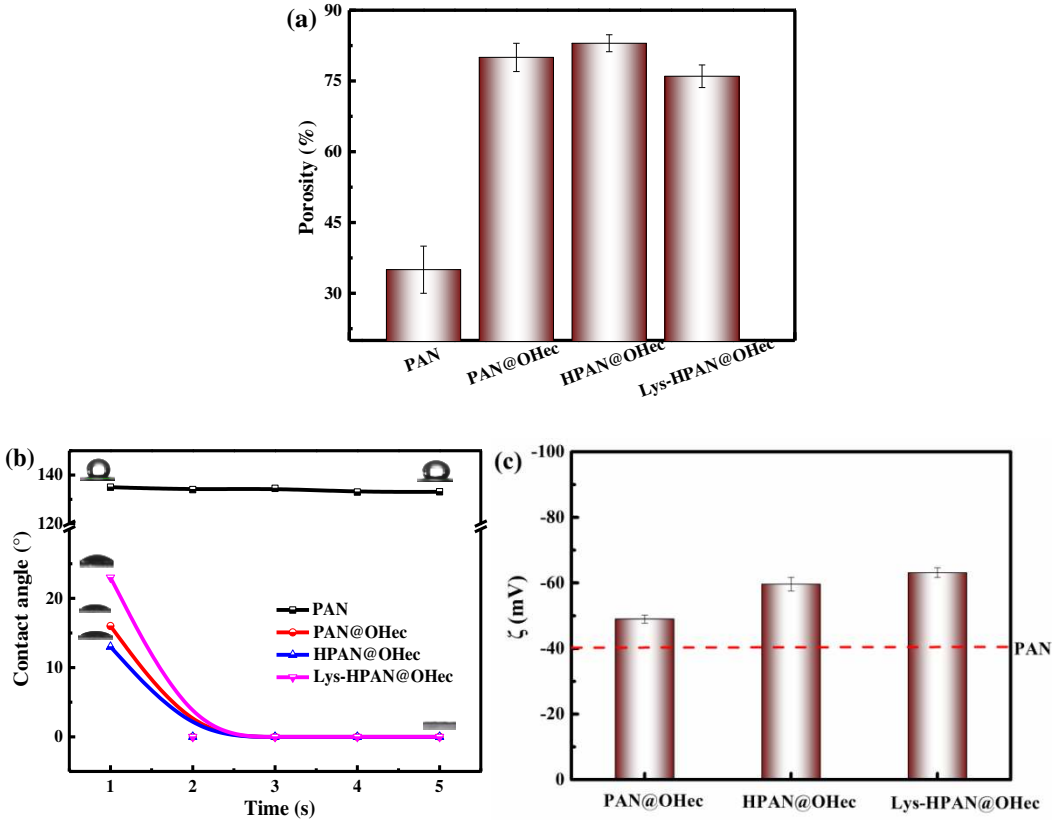

Fig. 6 Porosity (a), hydrophilicity (b) and the surface potential (c) of PAN membranes and modified membranes. Data are expressed as the mean ± SD of three independent measurements.

Normally, the pH value of the human body is fixed in a very narrow range between 7.35 and 7.45, so the charge properties of the membranes were measured by the flow potential of the sample at pH 7.4 to simulate the blood pH environment. As seen from Fig. 6c, all the membranes showed electronegativity at pH 7.4. For Lys-HPAN@OHec membranes, -NH_2 and -COOH groups of membranes surface changed the electromotive force, so the surface potential was large than one of PAN membranes. To sum up, this surface properties of Lys-PAN@OHec membranes would provide an excellent foundation for anti-protein adhesion and hemocompatibility.

Following the implantation of biomaterials or blood-contacting materials, the surface of materials will be coated with serum or plasma proteins [33, 34]. It is well known that the protein adsorption is the first event following blood-material contact

[35]. The protein adsorption is considered as an important factor causing membrane fouling. Moreover, protein fouling will make biomaterials susceptible to colonization and infection by bacteria [36]. In addition, bio-fouling is a major issue in membranes processes and decreases water flux or rejection. It was reported by literature that BSA had been used as model protein to investigate membrane bio-fouling process [37-39]. Fouling property of membranes were tested by the static and dynamic BSA adsorption experiments, respectively. As seen from Fig. 7a, the adsorption capacity for BSA of PAN membranes was about 26 mg/g, while the adsorption capacities of modified membranes obviously decreased. The BSA adsorption amount of Lys-HPAN@OHec membranes was decreased by 64 % compared to that of PAN membranes. The reason of these results was that PAN membranes with hydrophobic surfaces could produce strong hydrophobic interactions with BSA and more easily adhere BSA than hydrophilic membranes [38, 40]. Furthermore, the dynamic adsorption experiment was investigated by permeating pure water and BSA solution and shown in Fig. 7b. The water flux was higher than the BSA flux for whether PAN membranes or modified membranes. The BSA flux of Lys-HPAN@OHec membranes was increased compared to that of PAN membranes. The results indicated that Lys-HPAN@OHec membranes gave high resistance ability to BSA fouling due to the hydrophilic surfaces of membranes. The formation of hydration layer could hinder BSA or other biomacromolecules adhesion onto the surface of membranes. Hence, Lys-HPAN@OHec membranes exhibits more excellent anti-fouling performance for protein than pure PAN membranes.

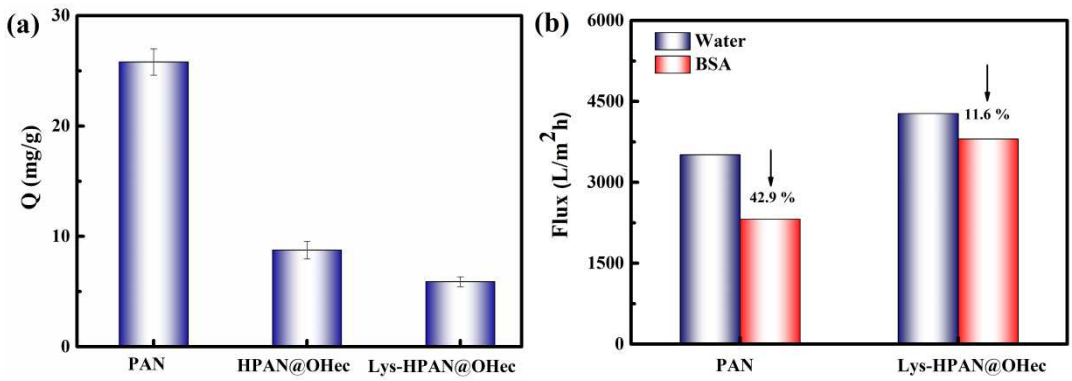

Fig. 7 The adsorption capacity (a) and flux (b) of BSA with various modified membranes.

Adsorption experiments

In this paper, two classical kinetic models were used to evaluate bilirubin adsorption behavior of particles. The models were fitted by the pseudo-first-order and the pseudo-second-order equations, expressed by Eqn (6) and Eqn (7), respectively [41,42].

$$\ln(q_e - q_t) = \ln q_e - k_1 t \tag{6}$$

$$\frac{t}{q_t} = \frac{1}{k_2 q_e^2} + \frac{t}{q_e} \tag{7}$$

where q_t (mg/g) and q_e (mg/g) are the adsorption capacity at time t (min) and equilibrium time, respectively. k_1 is the rate constant of the pseudo first-order kinetic, and k_2 is the adsorption rate constant of the pseudo-second order model.

The curves and fitted parameters of the adsorption kinetics were recorded and shown in Fig. 8 and Table 1, respectively. For Lys-HPAN@OHec membranes, the time equilibrium of adsorption kinetics was about 2 hours and the removal rate was over 90 % in Fig. 8a. However, the time reached equilibrium required almost 10 hours for PAN membranes, and the adsorption rate and capacity all decreased compared with Lys-HPAN@OHec membranes. As shown in Fig. 8, b, c and Table 1, both the adsorption processes were better in accord with the pseudo-secondorder model based on the correlation coefficient R^2.

The effect of temperature on bilirubin adsorption process was studied and presented in Fig. 9a. We can see that the adsorption capacity of Lys-HPAN@OHec membranes slightly increased with increasing temperature. According to the literature [43, 44], the conformational change occurred in the bilirubin adsorption process. The spatial conformation of bilirubin molecule converted from a *cis*-configuration to a *trans*-configuration in higher temperature. Therefore, more bilirubin molecule could be adsorbed and combined with Lys-HPAN@OHec membranes due to lower steric effect.

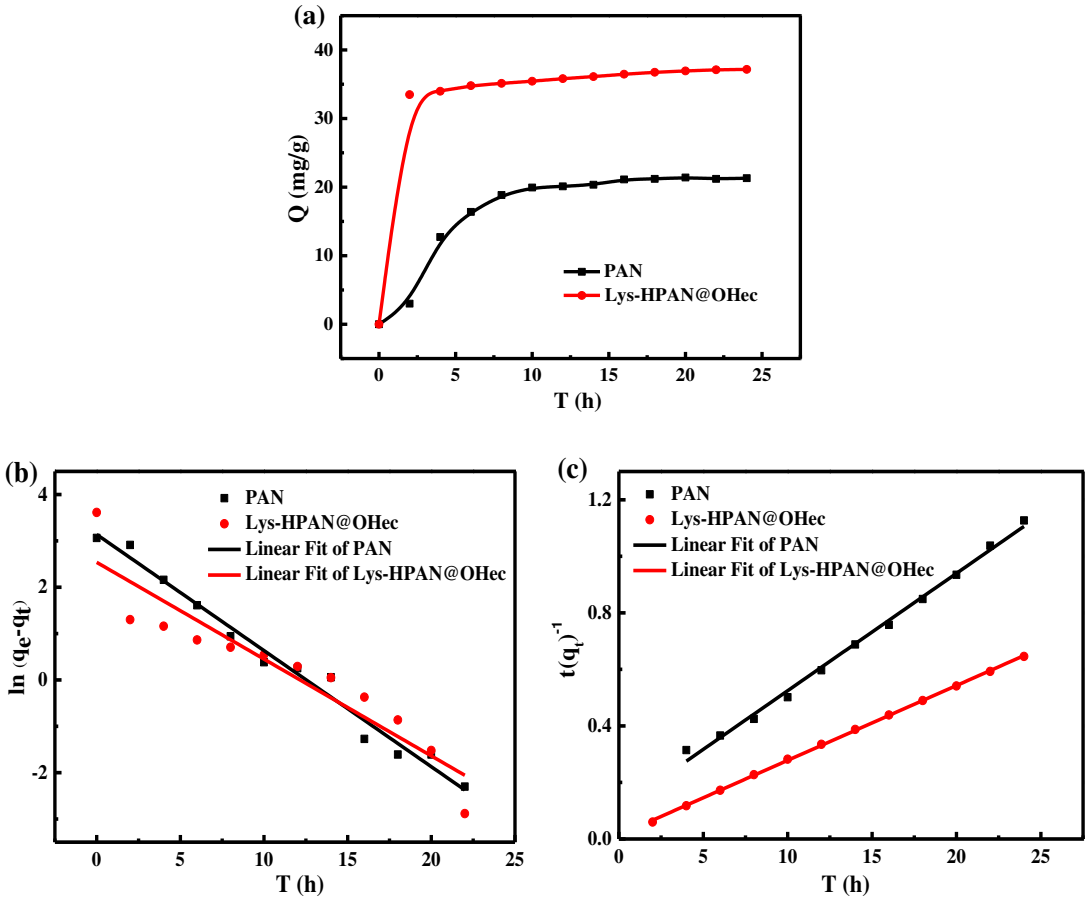

Fig. 8 The adsorption kinetics of Lys-HPAN@OHec and PAN membranes (a) , the pseudo-first order kinetic fitting plot (b) and pseudo-second order kinetic fitting plot (c).

Table 1 Kinetics parameters of Lys-HPAN@OHec membranes for bilirubin adsorption.

Sample	Pseudo-first order model		Pseudo-second order model	
	k_1 (h^{-1})	R_1^2	k_2 (g/mg h)	R_2^2
PAN	-0.251	0.979	0.042	0.995
Lys-HPAN@OHec	-0.209	0.861	0.026	0.999

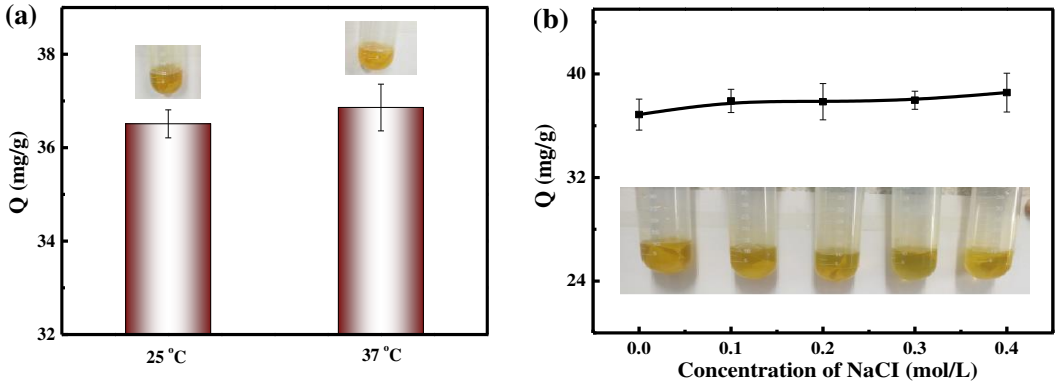

Fig. 9 The effect of temperature (a) and NaCl concentration (b) on the adsorption for bilirubin, the insert graph is the photo of bilirubin adsorption tests of Lys-HPAN@OHec membrane. (Initial bilirubin concentration: 200 mg/L; Temperature: 37 °C; Medium: PBS.) Data are expressed as the mean ± SD of three independent measurements.

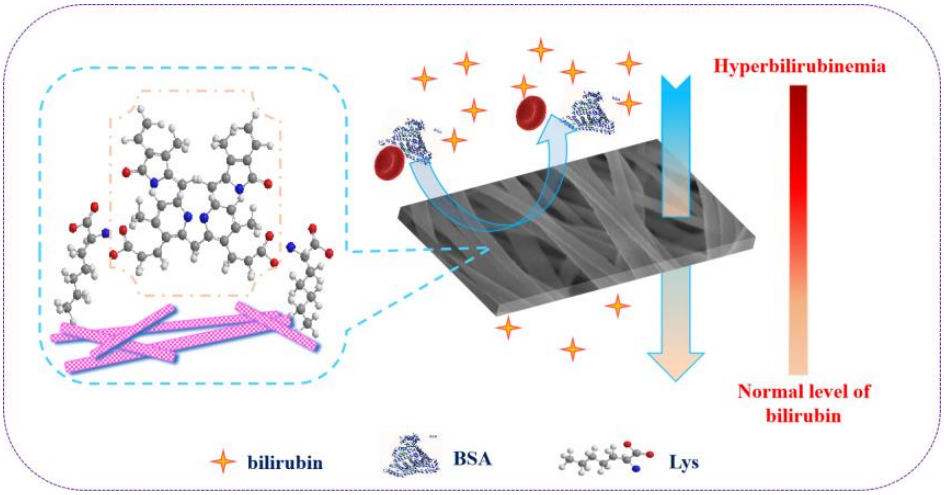

Fig. 10 Schematic illustrations of Lys-HPAN@OHec nanofiber membanes interaction with bilirubin and adsorption property.

The interactions between bilirubin and Lys-HPAN@OHec membranes mainly included electrostatic interactions or hydrophobic interaction. Lys-HPAN@OHec membane interaction with bilirubin was shown in Fig. 10. Hence, the ionic strength would be one of the major factors which affect on the adsorption process of membranes. The effect of ionic strength on bilirubin adsorption of Lys-HPAN@OHec membranes was investigated in Fig. 9b. As shown in figure, the adsorption capacity of membranes a little increased with increasing NaCl concentration in the solution. This result could be explained that the negative carboxyl ions of bilirubin attracted antiparticles around it to form an ionic atmosphere [45]. The ions in NaCl solution were driven to membranes surface, and bilirubin molecules were also assembled the

surrounding of membranes. Therefore, increased adsorption capacity was attributed to the increased interaction between bilirubin and membranes.

The adsorption isotherm is important to describe the process and characteristics of adsorption. As well known, the Langmuir model could describe the monolayer adsorption based on the assumption of adsorption homogeneity [46]. However, the Freundlich model was empirical and described the multi-layer adsorption taken place on a heterogeneous surface [17]. In this study, Langmuir and Freundlich adsorption isotherms were used to investigate bilirubin adsorption process.

The isotherm models were presented in Fig. 11, and Table 2 showed the correlation parameters for the Langmuir and Freundlich equation. The saturated adsorption amount of Lys-HPAN@OHec membranes for bilirubin was 64 mg/g. According to the correlation coefficients (R^2) shown in the table, R^2 of the Langmuir model was higher than one of the Freundlich model. The result indicated that the adsorption process of bilirubin for Lys-HPAN@OHec membranes matched the Langmuir model better than the Freundlich model.

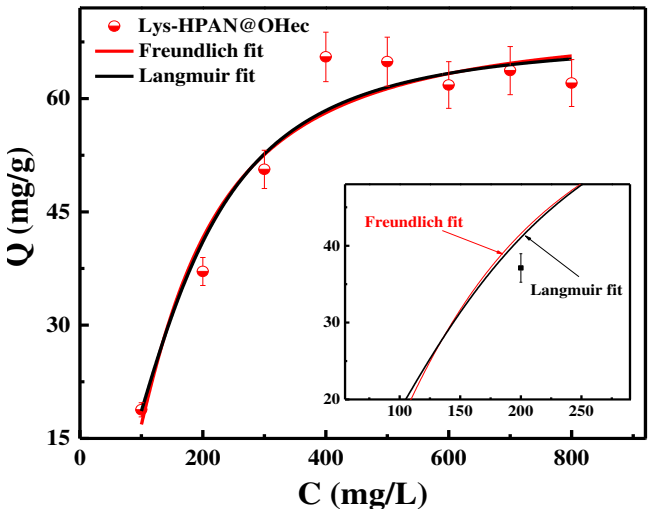

Fig. 11 Freundlich and Langmuir adsorption isotherm of Lys-HPAN@OHec membranes, the insert graph is the detail view of adsorption isotherm at concentration ranging from 100 to 300 mg/L.

Table 2 Langmuir and Freundlich isotherm constants of Lys-HPAN@OHec membranes

sample	Freundlich			Langmuir		
	n	K_f	R^2	q_m	K_L	R^2

Lys-HPAN@OHec	4.195	17.182	0.717	63.938	0.135	0.998

It is essential that the for bilirubin adsorption adsorbent can be used repeatedly with good performance. In order to investigate the reusability of Lys-HPAN@OHec membranes, we performed adsorption-desorption experiments for 5 cycles using NaOH as the eluent. As seen from Fig. 12a, the adsorption amount was about 32 mg/g after 5 cycles and decreased 10% than one of first cycle. Meanwhile, the surface morphology of membranes was unchanged after being treated with 0.1 M NaOH (Fig. 12b). In conclusion, Lys-HPAN@OHec membranes had good reusability and would be expected to use as an efficient for bilirubin adsorption adsorbent in clinical use.

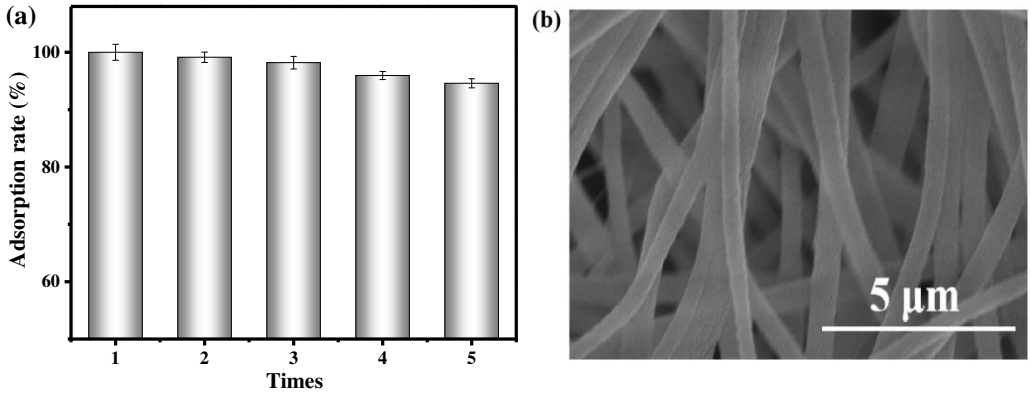

Fig. 12 (a) The adsorption-desorption cycles of Lys-HPAN@OHec membranes and (b) SEM image of membranes after 5 cycles.

Biocompatibility and hemocompatibility

The biomaterials contacting with blood environment for longterm should have excellent hemocompatibility and no procoagulant activity. Hemocompatibility, as an important activity for the hemodialysis materials, can be improved by means of modification or surface grafting reaction. Lys acted as a key modifier has been used to functionalized PAN membranes in order to improve their hemocompatibility. In this paper, the measurement of coagulation assay and hemolysis test were employed to evaluate the blood compatibility of membranes.

APTT is an indicator of the efficacy of the intrinsic and common plasma coagulation pathway, PT is assays evaluating the extrinsic pathway and common pathway of coagulation, while TT is used to test clot formation time taken for

thrombin conversion of fibrinogen into fibrin [47, 48]. Fig. 13a shows APTT, PT and TT values of PAN and Lys-HPAN@OHec membranes, respectively. For the value of APTT, the time of Lys-HPAN@OHec membranes was longer 4.0 s compared with raw PAN membranes. However, there was no significant changes in the values of PT and TT for Lys-HPAN@OHec compared with PAN. Above results suggested that modified PAN membranes did not activate the coagulation cascade or procoagulation activity.

Except for coagulation assay, hemolysis test was another parameter to evaluate the hemocompatibility. Fig. 13b showed the hemolysis values of Lys-HPAN@OHec and PAN membranes, while water and PBS were used as positive and negtive controls, respectively. According to ISO 10993-4 1999, materials with hemolysis values less than 5% are considered as safe, which could be used as blood-contacting materials [49]. The hemolysis rates of PAN and Lys-HPAN@OHec membranes were 44% and 2%, respectively. Compared with pure PAN membranes, the blood compatibility of Lys-HPAN@OHec membranes was obviously improved and could be considered as safe when contacted with blood environment.

For biomaterials or bioengineering materials, cytocompatibility is more important and regarded as the precondition in clinical application. The cytotoxicity of Lys-HPAN@OHec membranes was tested var MTT assay by L929 fibroblast cell with various cultured time. As shown in Fig. 13c, OD values of samples increased with increasing time. This result indicated that the cell viability had a steady increase and wasn't influenced by membranes. Meanwhile, there was no statistically significant difference in L929 cell activity between control group and samples in all culture time. The MTT results showed that Lys-HPAN@OHec membranes had good biocompatibility.

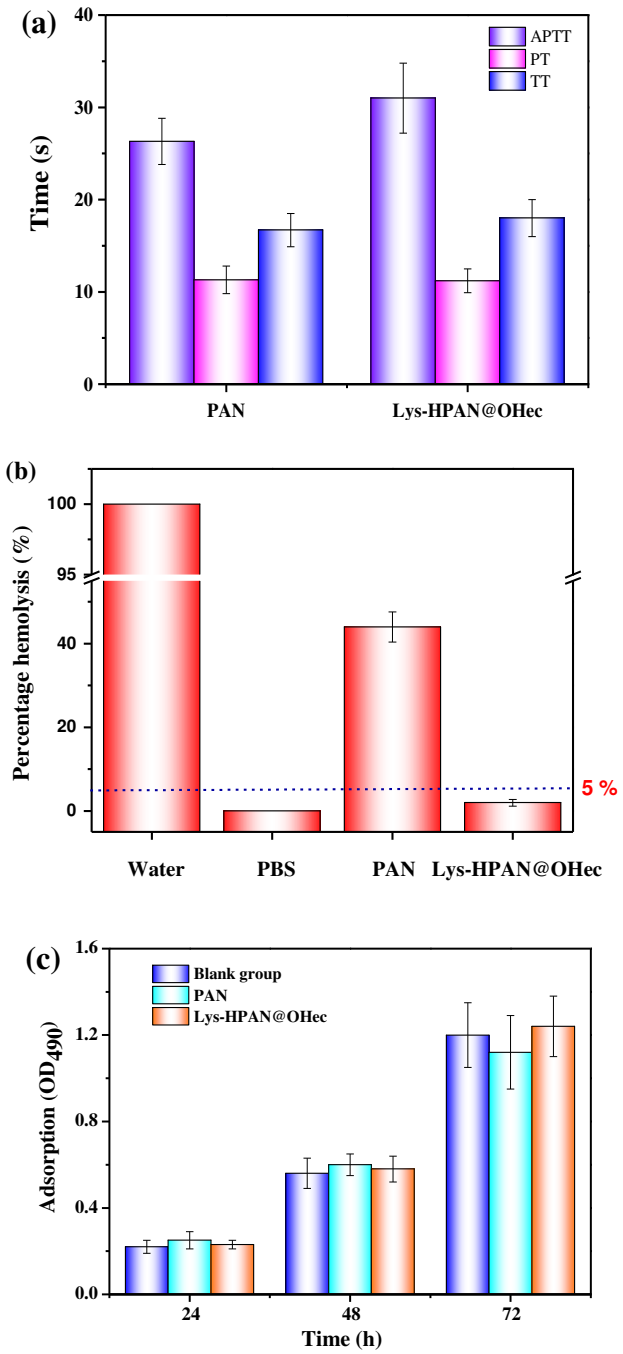

Fig. 13 (a) The APTT, PT and TT values of PAN and Lys-HPAN@OHec membranes. (b) Hemolysis assay for PAN and Lys-HPAN@OHec membranes, where water and PBS were used as positive and negative controls, respectively. (c) L929 cells proliferation in various culture time using MTT assay. All data are expressed as mean ± SD, n = 5.

Conclusion

In this study, PVP and OHec were doped with spinning solution to obtain the modified PAN membranes, and Lys-HPAN@OHec membranes were successfully synthesized via Lys grafting reaction. The Lys-HPAN@OHec membranes exhibited

significantly increased hydrophilicity, porosity and surface roughness than the pure PAN membranes. The adsorption performance of Lys-HPAN@OHec membranes for bilirubin exhibited short adsorption equilibrium time and high adsorption capacity. In addition, temperature and NaCl concentration had slight effects on the adsorption property for bilirubin of membranes. The adsorption kinetics and adsorption isotherms indicated that the adsorption processes were better in accord with the pseudo-secondorder model and the Langmuir model. Compared with PAN membranes, the hemolysis ratio of Lys-HPAN@OHec membranes was sharp decreased and the value of APTT was longer, these results indicated the excellent hemocompatibility of modified PAN membranes. In a word, this study provides an efficient and novel adsorbent for removing bilirubin in hemoperfusion.

Declarations

Funding Open Access funding provided by Tiangong University.

Competing interests The authors declare that they have no competing interests.

Availability of data and material Not applicable' for this section.

Code availability Not applicable' for this section.

Authors' contributions ML-designed and experimented, collected data, formal analysis, and wrote the manuscript; WZ-designed the experiment, corrected and revised the manuscript; HL and JZ-experimented and collected data; WZ and XM-material preparation.

Ethics approval Not applicable' for that section.

Consent to participate Not applicable' for that section.

Consent for publication Not applicable' for that section.

Acknowledgments This work was supported by National College Student Innovation and Entrepreneurship Training Program (201810058053). We would like to thank the Analytical & Testing Center of Tiangong University for providing characterization facilities.

References

1. Banks J, Montgomery D, Coody D, Yetman R (1996) Hyperbilirubinemia in the term newborn. Journal of Pediatric Health Care Official Publication of National Association of Pediatric Nurse Associates & Practitioners, 10: 228-230. https://doi.org/10.1016/S0891-5245(96)

90010-3.

2. Yan R, Han D, Ren J, Zhai Z, Zhou F, Cheng J (2018) Diagnostic value of conventional MRI combined with DTI for neonatal hyperbilirubinemia. Pediatr Neonatol 59: 161-167. https://doi.org/10.1016/j.pedneo.2017.07.009.
3. Kim JY, Lee DY, Kang S, Miao W, Kim H, Lee Y, Jon S (2017) Bilirubin nanoparticle preconditioning protects against hepatic ischemia-reperfusion injury. Biomaterials 133: 1-10. https://doi.org/10.1016/j.biomaterials.2017.04.011.
4. Baydemir G, Andaç M, Bereli N, Say R, Denizli A (2007) Selective removal of bilirubin from human plasma with bilirubin-imprinted particles. Ind Eng Chem Res, 46: 2843-2852. https://doi.org/10.1021/ie0611249.
5. Huang Y, Yuan ZP, Zhao D, Wang F, Zhang KX, Li YS, Wen YQ, Wang CT (2019) Polymyxin B immobilized nanofiber sponge for endotoxin adsorption. Eur Polym J, 110: 69-75. https://doi.org/10.1016/j.eurpolymj.2018.11.008.
6. Mller BR (2010) Effect of particle size and surface area on the adsorption of albumin bonded bilirubin on activated carbon. Carbon, 48: 3607-3615. https://doi.org/10.1016/j.carbon.2010.06.011.
7. Chen J, Han WY, Chen J, Zong WH, Wang WC, Wang Y, Cheng GH, Li CR, Ou LL, Yu YT (2017) High performance of a unique mesoporous polystyrene-based adsorbent for blood purification. Regen Biomater, 4: 31-37. https://doi.org/10.1093/rb/rbw038.
8. Ma KW, Yao DH, Chen JP, Li Y, Zhao CG, Liang GF (2018) Molecular synergistic strategy to fabricate bilirubin medical adsorbent material for hyperbilirubinemia hemoperfusion. Int J Polym Mater Po, 67: 727-738. https://doi.org/10.1080/00914037.2017.1376198.
9. Guo L, Zhang L, Zhang J (2009) Hollow mesoporous carbon spheres an excellent bilirubin adsorbent. Chem Commun, 40: 6071-6073. https://doi.org/10.1039/b911083f.
10. Zhao R, Li Y, Li X (2018) Facile hydrothermal synthesis of branched polyethylenimine grafted electrospun polyacrylonitrile fiber membrane as a highly efficient and reusable bilirubin adsorbent in hemoperfusion. J Colloid Interf Sci, 514: 675-685. https://doi.org/10.1016/j.jcis.2017.12.059.
11. Mokhtari-Shourijeh Z, Montazerghaem L, Olya ME (2018) Preparation of porous nanofibers from electrospun polyacrylonitrile/polyvinylidene fluoride composite nanofibers by inexpensive salt using for dye adsorption. J Polym Environ, 26: 3550-3563. https://doi.org/10.1007/s10924-018-1238-z.
12. Senthilkumar S, Rajesh S, Jayalakshmi A (2013) Biocompatibility and separation performance of carboxylated poly (ether-imide) incorporated polyacrylonitrile membranes. Sep Purif Techno, 107: 297-309. https://doi.org/10.1016/j.seppur.2013.01.041.
13. Kharaghani D, Jo YK, Khan MQ, Jeong Y, Cha HJ, Kim IS (2018) Electrospun antibacterial polyacrylonitrile nanofiber membranes functionalized with silver nanoparticles by a facile wetting method. Eur Polym J, 108: 69-75. https://doi.org/10.1016/j.eurpolymj.2018.08.021.
14. Yi SX, Sun S, Zhang YS, Zou YS, Dai FY, Si Y (2019) Scalable fabrication of bimetal modified polyacrylonitrile (PAN) nanofibrous membranes for photocatalytic degradation of dyes. J Colloid Interf Sci, 559: 134-142. https://doi.org/10.1016/j.jcis.2019.10.018.
15. Kim W, Shin DH, Jun J, Kim JH, Jang J (2017) Fabrication of shape-controlled palladium nanoparticle-decorated electrospun polypyrrole/polyacrylonitrile nanofibers for hydrogen

peroxide coalescing detection. Adv Mater Interfaces, 4: 1700573. https://doi.org/10.1002/admi.201700573.

16. Jiang HL, Kim YK, Arote R, Nah JW, Cho MH, Choi YJ, Akaike T, Cho CS (2007) Chitosan-graft-polyethylenimine as a gene carrier. J Control Release, 117: 273-280. https://doi.org/10.1016/j.jconrel.2006.10.025.
17. Xia BL, Zhang GL, Zhang FB (2003) Bilirubin removal by Cibacron Blue F3GA attached nylon-based hydrophilic affinity membrane. J Membr Sci, 226: 9-20. https://doi.org/10.1016/j.memsci.2003.08.007.
18. Ju J, He G, Duan ZJ, Zhao W, Liu YF, Zhang LL, Li YH (2013) Improvement of bilirubin adsorption capacity of cellulose cetate/polyethyleneimine membrane using sodium deoxycholate. Biochem Eng J, 79: 144-152. https://doi.org/10.1016/j.bej.2013.07.008.
19. Jiang X, Xiang T, Xie Y, Wang R, Zhao WF, Sun SD, Zhao CS (2016) Functional polyethersulfone particles for the removal of bilirubin. J Mater Sci Mater M, 27: 1-12. https://doi.org/10.1007/s10856-015-5642-9.
20. Wang WW, Zhang H, Zhang ZF, Luo MY, Wang YD, Liu QZ, Chen YL, Li MF, Wang D (2017) Amine-functionalized PVA-co-PE nanofibrous membrane as affinity membrane with high adsorption capacity for bilirubin. Colloids Surf B, 150: 271-278. https://doi.org/10.1016/j.colsurfb.2016.10.034.
21. Deere J, Magner E, Wall JG, Hodnett BK (2002) Adsorption and activity of proteins onto mesoporous silica. J Phys Chem B, 106: 7340. https://doi.org/10.1023/A:1022156405117.
22. Wu KK, Song X, Cui SY, Li ZT, Jiao YP, Zhou CR (2018) Immobilization of bovine serum albumin via mussel-inspired polydopamine coating on electrospun polyethersulfone (PES) fiber mat for effective bilirubin adsorption. Appl Surf Sci, 451: 45-55. https://doi.org/10.1016/j.apsusc.2018.04.242.
23. Shi W, Zhang F, Zhang G (2005) Adsorption of bilirubin with polylysine carrying chitosan-coated nylon affinity membranes. J Chromatogr B, 819: 301-306. https://doi.org/10.1016/j.jchromb.2005.02.018.
24. Li PY, Liu YY, Ma N, Zhang WQ (2018) L-Lysine functionalized polyacrylonitrile fiber: a green and efficient catalyst for knoevenagel condensation in water. Catal Let, 148: 813-823. https://doi.org/10.1007/s10562-017-2287-y.
25. Fu HL, Zhang W, Zhang H, Song SB, Li W (2016) Preparation and antibacterial activity of chitosan/organic laponite nanocomposites. J Inorg Mater, 31: 479-484. https://doi.org/10.15541/jim20150509.
26. Zhang W, Yue P, Zhang H, Yang N, Li JH, Meng JQ, Zhang QS (2019) Surface modification of AO-PAN@OHec nanofiber membranes with amino acid for antifouling and hemocompatible properties. Appl Surf Sci, 475: 934-941. https://doi.org/10.1016/j.apsusc.2018.12.179.
27. Aksoy OE, Ates B, Cerkez I (2017) Antibacterial polyacrylonitrile nanofibers produced by alkaline hydrolysis and chlorination. J Mater Sci, 52: 10013-10022. https://doi.org/10.1007/s10853-017-1240-1.
28. Xu SG, Liu YF, Yu Y, Zhang XT, Li YF (2020) PAN/PVDF chelating membrane for simultaneous removal of heavy metal and organic pollutants from mimic industrial wastewater. Sep Purif Technol, 235: 116185. https://doi.org/10.1016/j.seppur.2019.116185.

29. Kampalanonwat P, Supaphol P (2011) Preparation of hydrolyzed electrospun polyacrylonitrile fiber mats as chelating substrates: a case study on copper (II) ions. Ind Eng Chem Re, 50: 11912-11921. https://doi.org/10.1021/ie200504c.

30. Zhang G, Meng H, Ji S (2009) Hydrolysis differences of polyacrylonitrile support membrane and its influences on polyacrylonitrile-based membrane performance. Desalination, 242: 313-324. https://doi.org/10.1016/j.desal.2008.05.010.

31. Pan SF, Dong Y, Zheng YM, Zhong LB, Yuan ZH (2017) Self-sustained hydrophilic nanofiber thin film composite forward osmosis membranes: Preparation, characterization and application for simulated antibiotic waste water treatment. J Membr Sci, 523: 205-215. https://doi.org/10.1016/j.memsci.2016.09.045.

32. Shi Q, Su Y, Chen W, Peng J, Nie L, Zhang L, Jiang Z (2011) Grafting short-chain amino acids onto membrane surfaces to resist protein fouling. J Memb Sci, 366: 398-404. https://doi.org/10.1016/j.memsci.2010.10.032.

33. Latour RA (2005) Biomaterials: Protein-surface interactions [M].

34. Gristina AG (1987) Biomaterial-centered infection: microbial adhesion versus tissue integration. Science, 237: 1588-1595. https://doi.org/10.1007/978-1-4471-3454-1_25.

35. Roach P, Farrar D, Perry CC (2005) Interpretation of protein adsorption: surface-induced conformational changes. J Am Chem Soc, 127: 8168-8173. https://doi.org/10.1021/ja042898c.

36. Costerton JW, Stewart PS, Greenberg EP (1999) Bacterial biofilms: a common cause of persistent infections. Science, 284: 1318-1322. https://doi.org/10.1126/science.284.5418.1318.

37. Chan R, Chen V. (2004) Characterization of protein fouling on membranes: opportunities and challenges. J Membr Sci, 242: 169-188. https://doi.org/10.1016/j.memsci.2004.01.029.

38. Xu LC, Siedlecki CA (2007) Effects of surface wettability and contact time on protein adhesion to biomaterial surfaces. Biomaterials, 28: 3273-3283. https://doi.org/10.1016/j.biomaterials.2007.03.032.

39. Qi LB, Liu ZY, Wang N, Hu YX (2018) Facile and efficient in situ synthesis of silver nanoparticles on diverse filtration membrane surfaces for antimicrobial performance. Appl Surf Sci, 456: 95-103. https://doi.org/10.1016/j.apsusc.2018.06.066.

40. Ostuni E, Chapman RG, Holmlin RE, Takayama S, Whitesides GM (2001) A survey of structure-property relationships of surfaces that resist the adsorption of protein. Langmuir, 17: 5605-5620. https://doi.org/10.1021/la010384m.

41. Ahmed HA, Mubarak MF (2021) Adsorption of cationic dye using a newly synthesized $CaNiFe_2O_4$/chitosan magnetic nanocomposite: kinetic and isotherm studies. J Polym Environ, 29: 1835-1851. https://doi.org/10.1007/s10924-020-01989-0.

42. Ho YS, McKay G (1999) Pseudo-second order model for sorption processes. Process Biochem, 34: 451-465. https://doi.org/10.1016/S0032-9592(98)00112-5.

43. Shi W, Cao H, Song C, Jiang H, Wang J, Jiang S, Tu J, Ge D (2010) Poly (pyrrole-3-carboxylic acid)-alumina composite membrane for affinity adsorption of bilirubin. J Membr Sci, 353: 151-158. https://doi.org/10.1016/j.memsci.2010.02.048.

44. Denizli A, Kocakulak M, Piskin E (1998) Bilirubin removal from human plasma in a packed-bed column system with dye-affinity microbeads. J Chromatogr B Biomed Sci Appl, 707: 25-31. https://doi.org/10.1016/S0378-4347(97)00612-9.

45. Rustemeier O, Killmann E (1997) Electrostatic interactions and stability of poly-L-lysine covered polystyrene latex particles investigated by dynamic light scattering. J Colloid Interf Sci, 190: 360-370. https://doi.org/10.1006/jcis.1997.4875.

46. El-saied HAa, Motawea EAT (2020) Optimization and adsorption behavior of nanostructured $NiFe_2O_4$/Poly AMPS grafted biopolymer. J Polym Environ 28: 2335-2351. https://doi.org/10.1007/s10924-020-01774-z.

47. Jiang X, Zhou DX, Huang XL, Zhao WF, Zhao CS (2017) Hexanediamine functionalized poly (glycidyl methacrylate-co-N-vinylpyrrolidone) particles for bilirubin removal. J Colloid Interf Sci, 504: 214-222. https://doi.org/10.1016/j.jcis.2017.05.039.

48. Guo LM, Zhang JM, He QJ, Zhang LX, Zhao JJ, Zhu ZY, Wu W, Zhang J, Shi JL (2010) Preparation of millimeter-sized mesoporous carbon spheres as an effective bilirubin adsorbent and their blood compatibility. Chem Commun, 46: 7127-7129. https://doi.org/10.1039/c0cc02060e.

49. Peng ZH, Yang Y, Luo JY, Nie CX, Ma L, Cheng C, Zhao CS. (2016) Nanofibrous polymeric beads from aramid fibers for efficient bilirubin removal. Biomater Sci, 4: 1392-1401. https://doi.org/10.1039/c6bm00328a.

Supplementary Files

This is a list of supplementary files associated with this preprint. Click to download.

- GraphicalAbstract.docx
- Highlights.doc